

Surface quality improvement under low-frequency and high-amplitude vibration in rotational vibration-assisted incremental sheet forming

Oliver Lewthwaite¹, Jamie Booth¹, and Hui Long^{1*}

¹ The University of Sheffield, School of Mechanical, Aerospace and Civil Engineering, Sheffield, S1 3JD, United Kingdom

Abstract. Rotational Vibration-assisted Incremental Sheet Forming (RV-ISF) is a newly developed process variant that aims to improve upon conventional Incremental Sheet Forming (ISF), by the introduction of tool rotation-induced low-frequency and high-amplitude vibrations of deforming sheet. Different to existing ultrasonic vibration-assisted ISF processes with high-frequency and low-amplitude, the RV-ISF process introduces localised sheet vibrations under frequency typically below 300 Hz and amplitude from 5 to 100 μm . In this paper, an experimental study of the RV-ISF tool rotation-induced sheet vibrations on surface roughness reduction is presented. A trapezium test geometry using a helical toolpath is made by conventional ISF and RV-ISF processes with AA5251-H22 1 mm thickness sheets. Tool forming forces are measured by a piezoelectric force transducer and sheet vibrations are obtained by an Eddy current sensor. Optical measurements of surface roughness show that the RV-ISF tool is capable of reducing roughness of the sheet significantly and consistently across the entire sidewall of the trapezium samples, with a R_a reduction of up to 80% when compared to the conventional ISF tool.

Keywords: Incremental sheet forming; Vibration-assisted processing; High-amplitude, Surface roughness.

1 Introduction

ISF is an emerging die-less sheet metal manufacturing process which is best suited for bespoke to small batch size production, high-variability sheet metal products and rapid sheet metal prototyping. Due to being a dieless forming process, ISF can omit the die design, procurement and testing phases typically having long lead times, saving time and money in these applications [1]. Conventional ISF, namely single-point incremental forming (SPIF), utilises plane hemispherical forming tools, that follows a predefined computer numerically controlled (CNC) toolpath, deforming the sheet metal workpiece by applying localised pressure at the tool-workpiece interface causing progressive localised deformation. However, SPIF has several drawbacks:

- Poor surface quality;
- Low forming accuracy - lack of compliance of the final produced part to the designed part;
- Sheet thinning - reduction of sheet thickness due to material drawing out to cause fracture;
- Springback - geometric change to the part at the end of forming when the part is released.

Solutions to address these drawbacks have been investigated, the most prevalent being the introduction of localised heating to improve the formability of the workpiece material during forming, increasing the maximum strain that the sheet can undergo before sheet fracture. One such variation of SPIF that aims to implement localised heating is frictional-stir incremental sheet forming (FS-ISF). This variant produces localised heat by frictional heating generated by spinning the forming tool as it deforms the workpiece [2]. This allows for greater plastic deformation and the processing of materials that were formerly hard-to-form

with other ISF processes [3]. Consequently, hard-to-form materials, such as magnesium alloy, were able to be formed successfully with temperatures reaching 200°C [4].

One of the major factors that limits ISF industry adoption, such as within the automotive industry [1], are the challenges faced in producing an acceptable surface quality. Surface quality is characterised by small imperfections on the material surface that result in irregularities in surface texture, commonly measured by the average roughness, R_a . Several factors in the ISF processes affect the surface quality: spindle speed of the forming tool, feed rate, step depth, toolpath strategy, lubrication, the tool design geometry, and the forming angle of the part to be produced.

The tool spindle speed increases frictional heating contribution which improves the material formability. Hagan and Jeswiet [1] tested the effect of tool spindle speed on the surface finish using FS-ISF and a 12.7mm diameter hemispherical tool. It was found that the surface finish improved up to a certain spindle speed where after which the surface quality became worse, implying an optimal speed for a specific tool. On the other hand, the heating effect also influences lubrication and friction conditions which may introduce contrary effects on surface quality.

Hamilton and Jeswiet [5] investigated how the tool spindle speed affected the surface roughness and the formation of the 'orange peel', the surface texture on the non-contact side of a part formed by the tool. The occurrence of this surface texture was also described by Hosford and Caddell [6], providing guidelines for improvement of the non-contact face surface quality.

Friction has a major impact on the surface quality. Experimental data from Lu et al. [7] suggested that

* Corresponding author: h.long@sheffield.ac.uk

lower frictional resistance could achieve an improved surface quality and reduced forming load, using their ORB tool, an adaption of the SPIF tool that allowed the tool head to rotate freely. The coefficient of friction is difficult to determine in ISF processes as the horizontal force contains the frictional force but also the forming forces. As a substitute, a friction indicator μ^* was employed by both Lu et al. [7] and Xu et al. [8]. The friction indicator is defined as the ratio of horizontal force and vertical force, shown in Eq. (1):

$$\mu^* = \frac{F_H}{|F_V|} = \frac{\text{frictional force} + \text{forming force}}{|\text{vertical force}|} \quad (1)$$

Ultrasonic vibration forming was used in drawing processes and was found to be advantageous due to a reduction in flow stress and frictional forces at the die-workpiece interface, improving surface finish [9]. This principle was applied to ISF in the form of ultrasonic vibration assisted incremental sheet forming (US-ISF) [10], where an ultrasonic generator was added to the tool holder in SPIF that transmitted continuous high frequency and low amplitude vibrations into the tool. It was found that the vibrations were able to reduce the forming forces and improve formability.

Lu et al. [11] developed a rotation-induced vibration ISF by using tools that had their hemispherical head slightly offset from the spindle axis creating low frequencies of vibration but higher amplitudes than previous vibration assisted methods. It achieved force reductions similar to US-ISF without the requirement of additional equipment. With the introduction of vibration to the ISF process, an increased tool spindle speed will increase the vibration frequency therefore its effect is important. A rosette tool concept, by cutting short grooves on tool heads, was developed to produce low frequency vibrations [12], the process was named as rotational vibration-assisted ISF (RV-ISF), achieving significant forming force reductions and formability improvement in forming an magnesium alloy. A follow-on study also showed improvement on surface quality of aluminium parts by RV-ISF [13].

In this study, an optimised design of the rosette-type tool is developed, with six long-grooves on the tool head, named as T6. The effect of low-frequency and high-amplitude vibrations on surface quality is evaluated. The experimental tests of various ISF processes, including SPIF, FS-ISF and the newly developed RV-ISF, are performed to investigate variations of the forming forces, temperature increases, friction indicator and surface roughness, and the effects of two tool designs and tool spindle speed on the surface quality.

2 Methods and procedures

A CNC milling machine is used for the experimental tests. The sheet workpiece of aluminium alloy AA5251-H22 is sized in 150x150 mm with sheet thickness of 1mm. The test geometry is a trapezium of 50° wall angle and the toolpath generated for the test geometry has a step depth of 0.3 mm. All tests are conducted by using the tool feed rate of 1000 mm/min. In total six tests are

conducted using two different tools under different tool rotational speeds. The details of the experimental plan are shown in Table 1.

Table 1 Experimental plan of SPIF, FS-ISF, RV-ISF

Test No.	Tool	Rotational speed (rpm)	ISF process
1	T0	0	SPIF
2	T0	2000	FS-ISF
3	T0	3000	FS-ISF
4	T6	2000	RV-ISF
5	T6	2666.6	RV-ISF
6	T6	3000	RV-ISF

2.1 Tool designs for FS-ISF and RV-ISF tests

Two different tools are selected to compare their performance in improving the surface finishing under different tool spindle speeds. T0 tool with a hemispherical shape, as the conventional tool in SPIF, is tested. When the T0 tool is rotated, it generates frictional heating at the contact area between the tool and sheet surfaces; this setup enables FS-ISF. However there is no rotation-induced vibration generated by using the T0 tool. The T6 tool is designed with six long grooves on the tool head and an offset of 0.06 mm to the rotational axis of the tool. Compared to the short-grooved rosette tools in our earlier study in [12], the idea of the long-grooves is to enable the vibration effect to take place earlier in the process. The T6 tool is designed to generate low frequency and high amplitude vibrations when the tool is under rotation. This setup enables RV-ISF tests.

During the test, the tool forces and sheet temperature are measured by using a 3-component piezoelectric load cell and infrared thermal camera, as shown in Fig.1. The sample rate of the force measurements is made to be 3 times greater than the impacts per second of the tool on the sheet surface of the workpiece. To measure the sheet vibrations while the grooved tool is in contact with the sheet, an Eddy current sensor is positioned at 1 mm to the wall of a pyramid test piece of 40° degree to measure sheet vibration frequencies and amplitudes at different forming depths of the pyramid geometry.

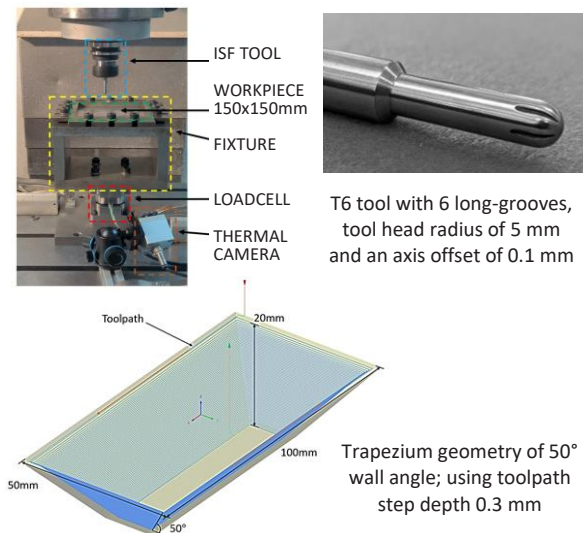


Fig. 1. RV-ISF of trapezium geometry by T6 tool

2.2 Surface roughness measurement

Optical measurements of surface roughness of the formed trapezium parts are conducted by using Alicona SL Infinite Focus-SL. These measurements are taken from 10 mm wide slices of the formed sample, cut from the long wall sections of the trapezium test piece using EDM (electrical discharge machining) wire cutting. The slices are then flattened out on the worked section and readings are recorded, gathering the *Ra* values. The slices have two different measurements taken, firstly ten 4mm profile surface roughness measurements, distributed randomly across the measurement window to gather a random average reading; secondly ten 3mm profile surface roughness measurements taken from the last 3 mm of the bottom surface of the trapezium test piece. The measurements from the slices are illustrated in Fig.2.

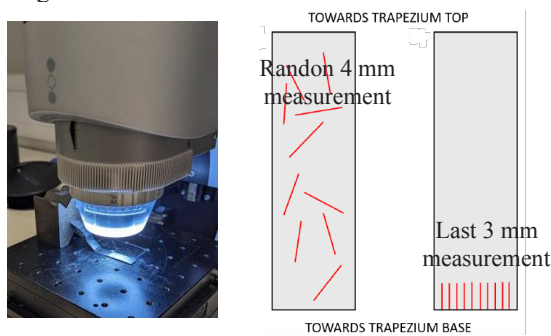


Fig. 2. Alicona surface roughness measurement methods

3 Results and discussion

In this section, the results of the tool vertical and horizontal forces and temperature measurements are presented first, followed by analysing the measurement results of vibration frequencies and amplitudes, and finally an evaluation of surface roughness.

3.1 Results of force and temperature variations

Fig.3 shows a comparison of the tool vertical and horizontal forces under tool spindle speed of 2000 rpm when using T0 and T6 tools respectively. The forces vary cyclically when the tool moves over the 4 different sections of the trapezium geometry, being greatest at the corners. Employing the T6 tool it reduces the vertical forming force significantly in comparison with that using the T0 tool.

Table 2 Force, friction indicator and temperature

Test No.	Maximum vertical force (N)	Average friction indicator	Change in sheet temperature (°C)
1	797.3	0.2056	2.7
2	710.9	0.1202	5.9
3	728.3	0.1326	30.1
4	507.0	0.1550	3.2
5	485.2	0.1605	5.1
6	490.4	0.1542	22.7

The maximum vertical forming force of the tool and temperature change of the deforming sheet for each test are summarised in Table 2. The temperature increases are limited when the tool spindle speed is below 2000 rpm but reach a maximum increase of 30°C for T0 tool and 22°C for T6 tool under 3000 rpm. Fig.4 compares the maximum vertical forming forces under different conditions. It can be seen that T6 tool reduces the vertical force by a maximum of 37% than that by using T0 tool. It is clear that the effect of sheet temperature increases on the vertical force reduction is minimal. The significant reduction of the vertical force is a result of the rotation-induced vibration of the sheet workpiece by employing T6 tool, which is absent for T0 tool.

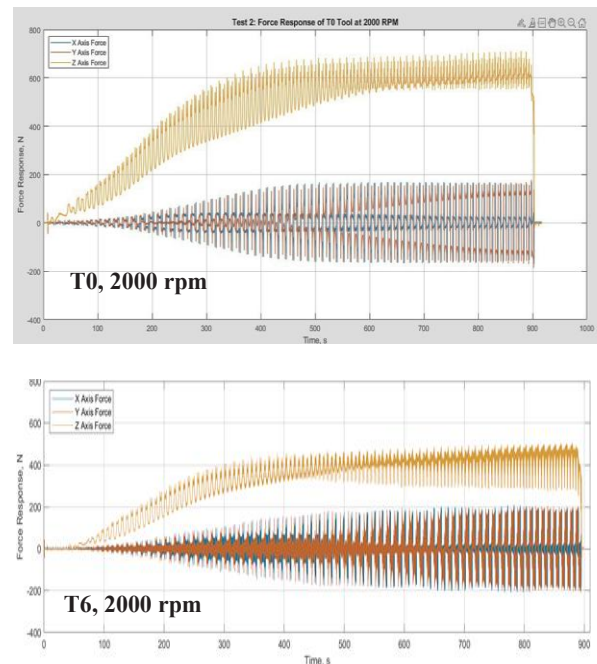


Fig. 3. Forces measured under 2000 rpm by T0 & T6 tool

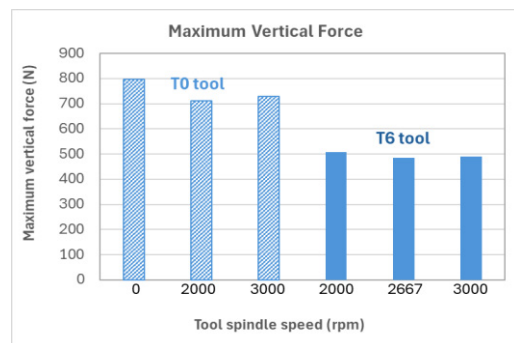


Fig. 4. Comparison of maximum vertical forces by T0 & T6

3.2 Analysis of vibration amplitudes

The displacement data measured by using the Eddy current sensor is processed using a fast Fourier transformation, allowing for the sheet vibrational behaviour to be analysed. As can be seen in Fig.5, under 2000rpm tool spindle speed, at frequency 33Hz (one vibration for every tool rotation), a high amplitude of 107µm is observed which is caused by the axis-offset of T6 tool. There is a small amplitude vibration of 6.6µm at 200Hz (six vibrations for every tool rotation) which

is the result of the impacts of six grooves of the tool head on the deforming sheet. Similar observations are found when T6 tool is under the spindle speed of 3000 rpm; a high amplitude vibration of 102 μm at 50 Hz due to the tool axis-offset and a small amplitude vibration of 7.3 μm at 300 Hz due to the six grooves of the tool.

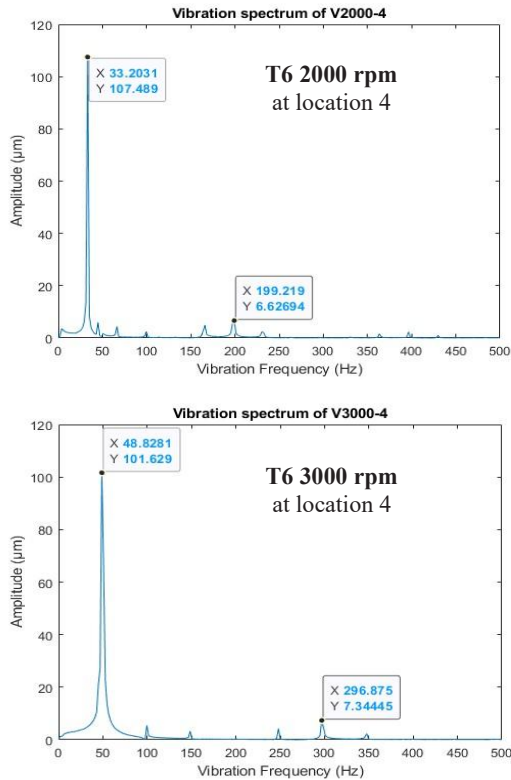


Fig. 5. Vibration spectrums by T6 tool, 2000 & 3000 rpm

To ascertain the tool rotation-induced sheet vibrations are localised, the Eddy current sensor takes readings while the T6 tool moves from the top to the bottom of the pyramid test piece. Fig.6 shows the readings at different locations of the part wall where the sensor is located nearby (sensor measurement points) and away from the sensor. It can be observed the maximum amplitude of vibrations is at the sensor measurement location, varying when the tool moves closer to the sensor location. When the tool moves to the opposite wall of the pyramid, away from the wall of the pyramid where the sensor is located, the amplitudes are

around 20 μm (orange dots), much smaller than the maximum amplitudes of around 100 μm (blue dots). These observations and analysis confirm that the tool rotation-induced vibrations of the deforming sheet are localised at adjacent areas of the tool-sheet contact.

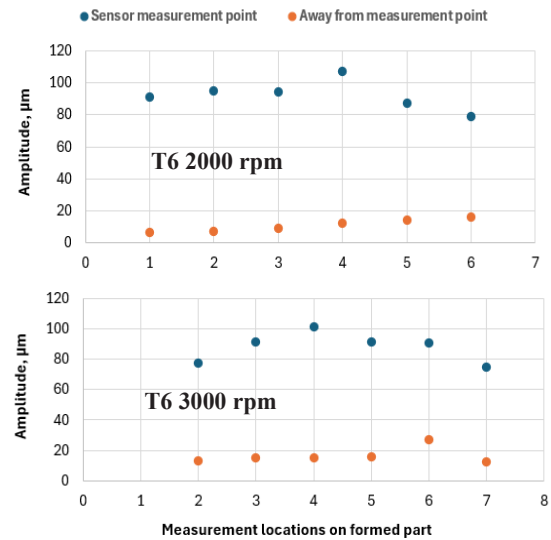


Fig. 6. Variations of vibration amplitudes by T6 tool

3.3 Analysis of friction indicator

The friction indicator, shown in Eq.1, is calculated by using the measured vertical and horizontal forces for each test. As discussed in Introduction, the frictional force is contained within the horizontal force that also includes the forming forces. The test piece of the trapezium geometry includes the short-wall and long-wall sections and corners, as shown in Fig.7. The long-wall sections (100 mm sides) provide a stable value of friction indicator. Thus, 10 periods of the long wall section, spread evenly across a test over forming time, are used to produce the average friction indicator. As can be seen in Fig.8, the friction indicators by T0 tool under 2000 and 3000 rpm are lower than that by T6 tool, this is because the vibrations generated by T6 create greater variations of the horizontal force, contributing to a higher friction indicator. However, as observed and discussed in [14], the friction indicator may not be an accurate parameter to evaluate the frictional condition in ISF processes. Better methods need to be developed to accurately determine the coefficient of friction in ISF.

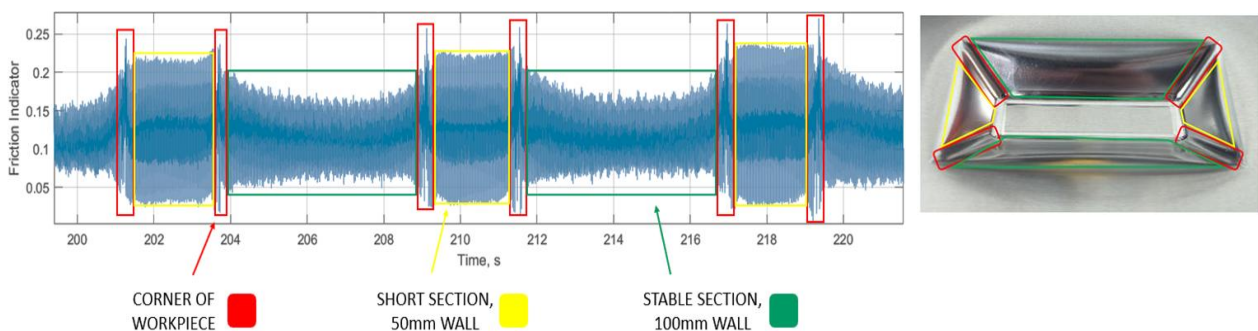


Fig. 7. Stable friction indicator by selecting the data from long-wall sections of the trapezium geometry

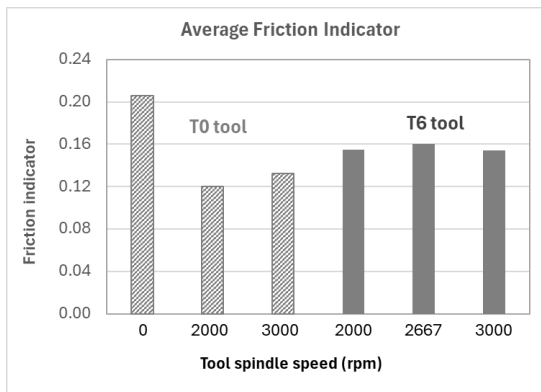


Fig. 8. Comparison of friction indicator by using T0 & T6

3.4 Analysis of surface roughness

By using the method for surface roughness measurements described in Section 2.2 and shown in Fig.2, Fig.9 compares the results of surface roughness measurement results, R_a , under different test conditions. By comparing SPIF (T0 without tool rotation) and FS-ISF (T0 with tool rotation), it can be seen that the surface roughness is reduced when T0 tool is under spinning speed of 2000 rpm but increased under 3000 rpm. This is likely due to the increased friction over time due to the accumulation of the frictional heating leading to a higher temperature increase of the sheet workpiece, to 30°C under 3000 rpm by T0.

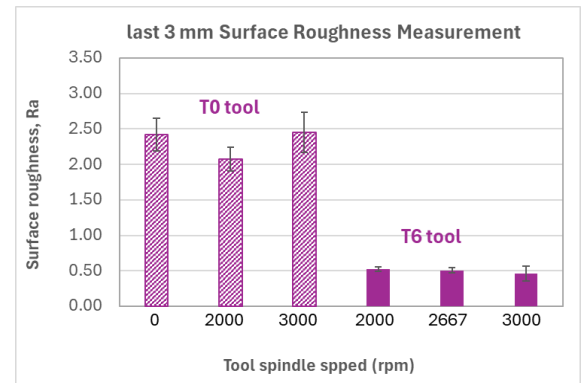
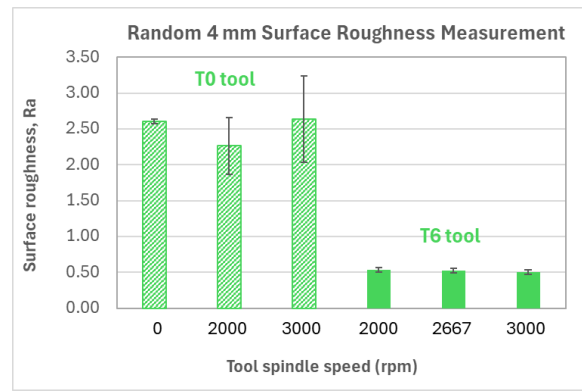


Fig. 9. Comparison of average surface roughness by T0 & T6

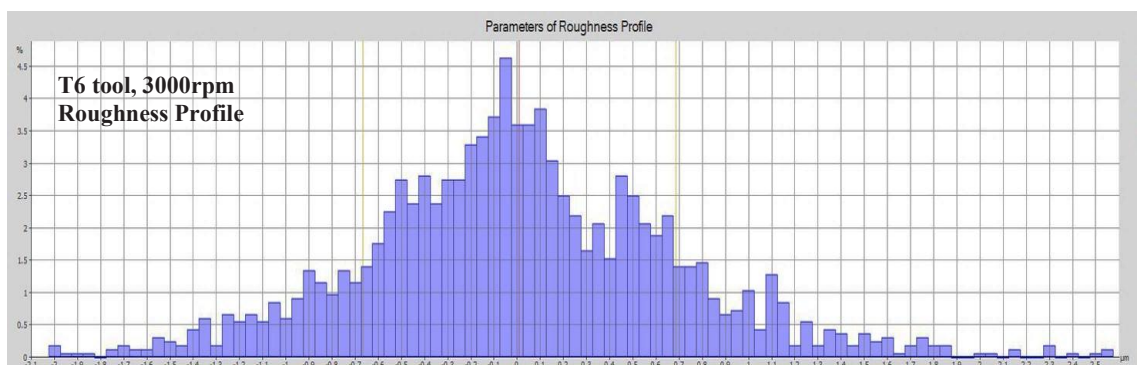
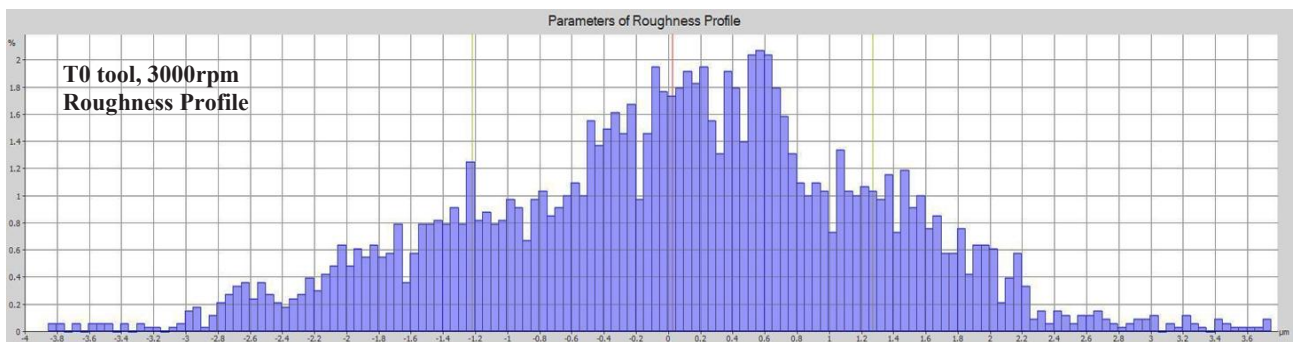
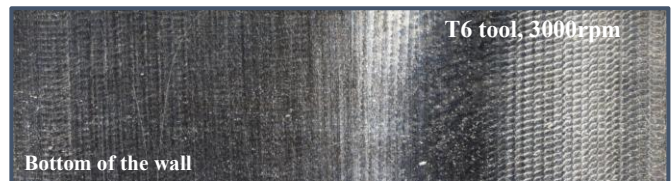


Fig. 10. Surface texture of the wall section and distribution of the surface roughness profile by T0 and T6 under 3000rpm

As shown in Fig.9, comparing FS-ISF by T0 tool (without vibrations) and RV-ISF by T6 tool (with vibrations), the average values of surface roughness, R_a , are significantly reduced by T6. Across all tool spindle speeds tested, comparing the performance of T0 and T6, the reduction of the average surface roughness values by T6 is observed, with a maximum reduction being about 80%, indicating the design of T6 tool has capability to improve the average surface quality by employing RV-ISF processing. The surface finish produced by the T6 tool also appears to be more consistent across the wall section, with only an average roughness increase of 4.34% when comparing its last 3mm value to the randomly distributed 4mm roughness value.

The surface texture of a wall section by using T0 and T6 tools under spindle speed of 3000 rpm is compared in Fig.10. By using T0, the surface texture becomes slightly smoother from the top section to the bottom of the wall of the formed trapezium pieces. While using T6, it is visible on the measured samples that the occurrence of ‘fish-scale’ surface texture at the top section of the wall, which occurs at the beginning of the RV-ISF process. This is likely resulted from the impacts of the tool grooves on the sheet surface before the vibration effect takes place. Localised vibrations of the deforming sheet can only be established after the sufficient forming depth is reached to enable the full contact of the grooved tool head with the angled wall of the trapezium geometry. After the very initial stages of forming, the ‘fish-scale’ texture almost disappears and the surface becomes smoother at the bottom of the wall.

The distribution of surface roughness profile by T0 and T6 tools are also compared, as shown in Fig.10. The variation of roughness values by T0 is considerably greater than that by T6. For T0, the roughness values are largely spread over a greater range between the maximum and minimum roughness values. For T6, the majority of the roughness values is centred within a smaller range, producing a more evenly distributed roughness profile. The design of narrow and long grooves on the tool head may have improved the lubrication by containing and releasing the oil onto the sheet periodically due to the effect of the vibrations.

4 Conclusions

This study experimentally investigates the effect of low frequency and high amplitude vibrations on surface quality of ISF processes, including SPIF, FS-ISF and the newly developed RV-ISF by developing a new grooved tool T6. The following conclusions may be drawn:

(1) The T6 tool in RV-ISF is capable of reducing the average surface roughness significantly and consistently across the entire sidewall of the samples, with a R_a reduction of up to 80% when compared to T0 tool in FS-ISF. This effect is the result of a more evenly distributed surface roughness profile.

(2) Vibration measurements of the deforming sheet show that the high amplitude vibrations of $\sim 100 \mu\text{m}$ is caused by the offset of the tool to the rotational axis and the low amplitude vibrations of $\sim 7 \mu\text{m}$ is caused from the grooves on the tool. The vibration frequencies are low,

within 33~300Hz under tool spindle speeds of 2000 and 3000 rpm by using T6 tool.

(3) Forming forces when using the T6 tool are reduced by a maximum of 37% than that by the T0 tool due to the high amplitude and low frequency vibrations. Temperature increases in both FS-ISF and RV-ISF are very small, confirming that the forming force reduction is a result of tool rotation-induced vibrations of the deforming sheet rather than the thermal softening of the material.

Acknowledgements

The authors acknowledge the financial support received from the UK Engineering and Physical Sciences Research Council (EPSRC) through project grants EP/W010089/1 and EP/T005254/1.

References

1. E. Hagan, J. Jeswiet, Proc IMechE Part B: J Engineering Manufacture, **218**, 10 (2004)
2. M. Otsu, H. Matsuo, M. Matsuda, K. Takashima, Steel Res. Int., **81**, 9 (2010)
3. Z. Wang, S. Cai, J. Chen, J. Mat. Proc. Techno., **277** 116488 (2020)
4. J. Park, J. Kim, N. Park, Y. Kim, Metallurgical and Materials Transactions A, **41** (2010)
5. K. Hamilton, J. Jeswiet, CIRP Annals, **59**, 1 (2010)
6. W. F. Hosford, R. M. Caddell, Metal forming: mechanics and metallurgy, Cambridge university press, 2011
7. B. Lu, Y. Fang, D. K. Xu, J. Chen, H. Ou, N. H. Moser, J. Cao, International Journal of Machine Tools and Manufacture, **85** (2014)
8. D. Xu, W. Wu, R. Malhotra, J. Chen, B. Lu, J. Cao, International Journal of Machine Tools & Manufacture, **73** (2013)
9. T. Jimma, Y. Kasuga, N. Iwaki, O. Miyazawa, E. Mori, K. Ito and H. Hatano, J. of Materials Processing Technology, **80-81** (1998)
10. S. Amini, A. Hosseinpour Gollo and H. Paktinat, The Int. J. of Advanced Manufacturing Technology, **90** (2017)
11. B. Lu, Z. Li, H. Long, F. Chen, J. Chen and H. Ou, Procedia Engineering, **207** (2017)
12. H. Long, W.X. Peng, Z.D. Chang, H. Zhu, Y.J. Jiang, Z.H. Li, J. of Materials Processing Technology, **118311-118311** (2024)
13. W. X. Peng, E. Hurtado Molina, F. A. Solum, J. Booth and H. Long, in Proceedings of the 14th International Conference on the Technology of Plasticity - Current Trends in the Technology of Plasticity, ICTP, 24-29 September 2023, France (2023)
14. Z. Chang, W.X. Peng, H. Long, J. of Materials Processing Technology, **118692-118692** (2024)